Semi-Tomographic Gamma Scanning Technique for Non-destructive Assay of Radioactive Waste Drums

Weiguo GU, Kaiyuan RAO, Dezhong WANG, Jiemei XIONG

Abstract—**Segmented gamma scanning (SGS) and tomographic gamma scanning (TGS) are two traditional detection techniques for low and intermediate level radioactive waste drum. This paper proposes one detection method named semi-tomographic gamma scanning (STGS) to avoid the poor detection accuracy of SGS and shorten detection time of TGS. This method and its algorithm synthesize the principles of SGS and TGS. In this method, each segment is divided into annual voxels and tomography is used in the radiation reconstruction. The accuracy of STGS is verified by experiments and simulations simultaneously for the 208 liter standard waste drums which contains three types of nuclides. The cases of point source or multi-point sources, uniform or nonuniform materials are employed for comparison. The results show that STGS exhibits a large improvement in the detection performance, and the reconstruction error and statistical bias are reduced by one quarter to one third or less for most cases if compared with SGS. The detection time of STGS is longer than SGS, but shorter than TGS, which indicates that STGS has the good overall performances for non-destructive assay of radioactive waste drums.**

Index Terms—**STGS, Non-destructive Assay, Radioactive Waste**

I. INTRODUCTION

Radioactive wastes have to be detected before the intermediate treatment and final storage because they should meet the acceptance criteria defined by national regulatory and management authorities. In order to estimate the amount and categories of the radioactive nuclides inside the waste packages, non-destructive assay (NDA) techniques, especially gamma scanning techniques including segmented gamma scanning (SGS) and tomographic gamma scanning (TGS) are widely used.

The first SGS and TGS systems were both established by Los Alamos National Laboratory respectively in early 1970s [1] and 1990s [2]. SGS divides the waste drum into several axial segments and assumes that filler materials and radioactive sources are uniformly distributed in each segment, but large systematic errors normally appear in the case of nonuniform distribution. TGS further divides the segments into several voxels and reconstructs the three-dimensional distribution of radioactive sources using tomographic method. The detection accuracy of TGS is improved greatly [3], but the detection process becomes complicated which leads to the detection time much longer than SGS.

In last two decades, some efforts have been made in order to improve the detection accuracy of SGS and reduce detection time of TGS. In real waste drum, the radioactive sources usually are not distributed uniformly, and the area containing comparatively large radiation is called "hotspot". In this situation, rotating the waste drum during the measurement is one method to reduce the nonuniformity. If the rotation is at a constant speed within a long time, the point source can approximate the ring source. Anh studied the method to reconstruct the ring source, but the study aimed at one segment and assumed the material was uniform [4]. Another method is to reconstruct the radius of the ring source firstly and calibrate the detection efficiency according to the ring radius [5]. This method assumes multi-point sources as point source, so the accuracy is not good in the case of multi-point sources. In addition, there are some studies using statistical method of analyzing angular dependent count rate distribution to improve the accuracy of SGS [6], [7], however the results are not ideal when there are more than three same point isotopes simultaneously in one segment. As to TGS, reducing the voxel number in one segment is an effective way to shorten detection time. In order to avoid voxels reduction leading to the decrease of detection accuracy, adaptive dynamic voxels are applied in the reconstruction calculation where the voxels are refined around the radioactive sources [8], [9]. By this method, the detection time of TGS is shortened by half by compared with the case of fixed voxels, but the reliability of the algorithm is not studied absolutely. Until now, these problems of SGS and TGS have not been solved absolutely.

This paper presents one method named STGS and its algorithm which synthesizes the principles of SGS and TGS. In this method, the waste drum rotates and the point source is regarded as the ring source. The segment is divided into several annular voxels, and tomography is used in reconstructing the radial distribution of radionuclides and activities within these annular voxels. Because the voxel division in one segment is one-dimensional instead of two-dimensional division in TGS, this method is called as semi-tomographic gamma scanning (STGS).

II. DETECTION PRINCIPLE

For the low and intermediate level gamma-contaminated 208 liter waste drums, the schematic of gamma scanning detection system is shown in figure 1. The instrument employs a single shielded and high purity germanium (HPGe) detector. The density of the filler materials can be estimated by weighting the waste drum and by transmission reconstruction depending on the attenuation of gamma rays emitted by transmission source where typically Eu-152 is employed.
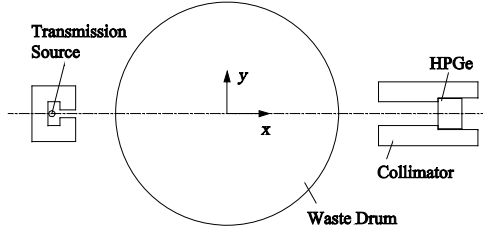
(a) Layout in x-y plane
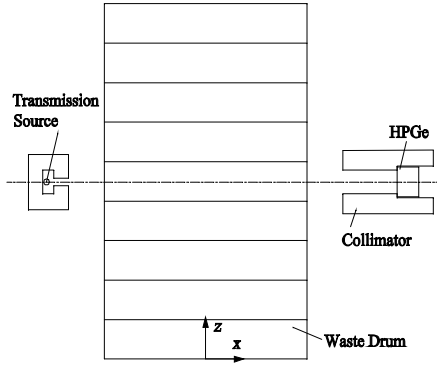
(b) Layout in x-z plane

Fig. 1. The schematic of gamma scanning detection system.

Conventional SGS divides the waste drum into several segments which is according to the dimension and position of detector's collimator. The detector is placed toward the waste drum which is rotating continuously. The assay is performed segment by segment in sequence. The transmission gamma rays penetrate the segmental materials and are counted by the detector. According to Beer's law, this transmission measurement is described by

$$\frac{C_k}{C_{k,0}} = \exp\left(-\mu_k D\right)$$

(1)

Where, $C_{k,0}$ is the count rates from the transmission source when the drum is empty, C_k is the count rates after filler material's attenuation in the k-th segment, μ_k is the attenuation coefficient of the material in the k-th segment, D is the diameter of the waste drum.

Before emission measurement, the detection efficiency is calculated by adopting segmental volume source in calibration. The detection efficiency (E') depends on the geometric size, the position of detector, material density (ρ) and radionuclide energy (e). Emission measurement is described by

$$C_k = \alpha \sum_{n=1}^{N} A_n E'_{nk}\left(\rho, e\right)$$

(2)

Where, C_k is the count rates from emission source when the detector is positioned toward the k-th segment, A_n is the activity of one radionuclide in the n-th voxel, α is the branching ratio of gamma line whose characteristic energy is e. When whole measurements are finished, a group of linear equations are constructed consisting of K equations and N unknowns where K is the total number of detector positions and N is the total segments number. Solving the linear equations, the activities distributed in each segment can be obtained.

In order to resolve the problem of low accuracy of SGS caused by uniformity assumption in each segment, TGS further divides the segment into several voxels as seen in figure 2 and reconstructs the distribution of density and activity by tomography. Because of the large number of voxels, at least the same times of detections are required to close the voxels in solving linear equations. One method of TGS detection process is that the waste drum rotates a small angle step by step instead of continuously. When the rotation is stopped, detection is performed. Moreover, the detector and transmission source will both be translated eccentrically in y direction to obtain enough detections.
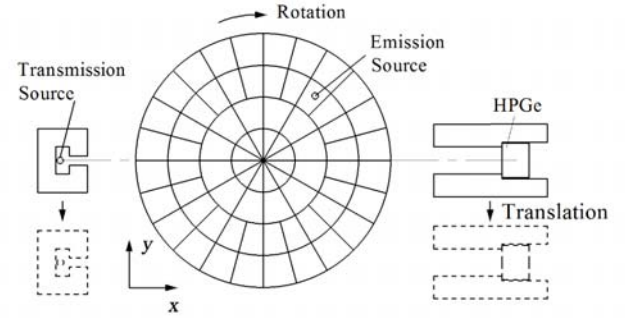

Fig. 2. The schematic of TGS voxels in the segment and detection process.

The transmission measurement of TGS is described by

$$\frac{C_{ijk}}{C_{ijk,0}} = \exp\left(-\sum_{n=1}^{N} \mu_n L_n\right)$$

(3)

Where, i, j, k denote the serial number of detector positions in circumferential, eccentric and vertical directions respectively; n denotes the serial number of the voxels in the waste drum and the total number is N; μ_n and L_n are the linear attenuation coefficient and gamma ray track length in the n-th voxel along the transmission route. It is worth noting that the group of

measurements should insure that each voxel has to be penetrated by transmission gamma rays at least once to conclude the attenuation coefficient in each voxel.

As to TGS emission measurement, point source is supposed to be positioned in the geometric center of a voxel, the measurement is described by

$$C_{ijk} = \alpha \sum_{n=1}^{N} \left[A_n E_{n,ijk}(e) \exp\left(-\sum_{n=1}^{N} \mu_n L_n \right) \right]$$ (4)

Where, C_{ijk} is the count rate of detector which is in the i-th circumferential, j-th eccentric and k-th vertical position; α is the branching ratio of gamma line; A_n is the activity of one radionuclide in the n-th voxel; $E_{n,ijk}$ is the detection efficiency of point source in the n-th voxel to detector without attenuation, and radionuclide energy is e; L_n is the track length within the n-th voxel of gamma ray along the route from the point source to detector.

For STGS, the waste drum rotates at a constant speed and each segment is divided into a small amount of annular voxels. Figure 3 shows four types of voxel division. The point source is supposed as the ring source because the waste drum keeps rotating. In each annular voxel, the filler material and radioactive sources are assumed to be distributed uniformly. Referring to the principle of TGS, the transmission and emission measurements of STGS is described by

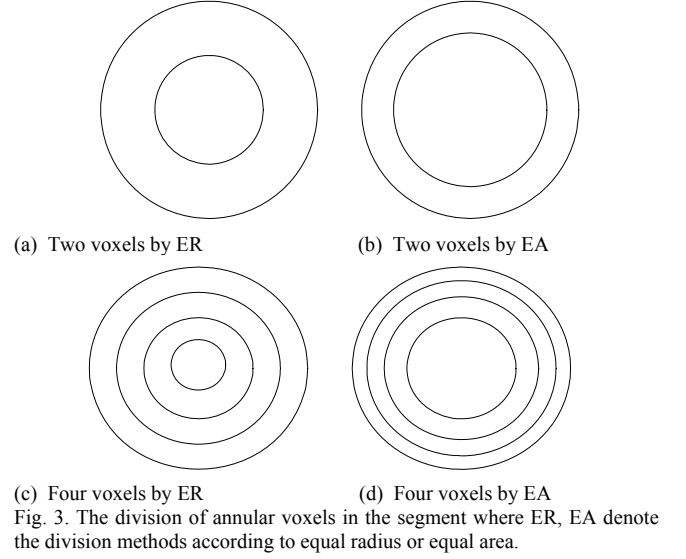$$\frac{C_{jk}}{C_{jk,0}} = \exp\left(-\sum_{n=1}^{N} \mu_n L_n \right)$$ (5)

$$C_{jk} = \alpha \sum_{n=1}^{N} \left\{ A_n E_{n,jk}(e) \exp\left(-\sum_{n=1}^{N} \mu_n L_n \right) \right\}$$ (6)

Where, j, k respectively denote the serial number of detector position in eccentric and vertical directions; n denotes the serial number of the annular voxel in the waste drum and the total number is N; C_{jk} is the count rates of the detector; $C_{jk,0}$ is the count rates in transmission measurement when there is no material attenuation; μ_n and L_n are the linear attenuation coefficient and gamma ray track length in the n-th annular voxel; A_n is the activity of one radionuclide in the n-th annular voxel; $E_{n,jk}$ is the detection efficiency of annual volume source in the n-th voxel to detector without attenuation.

## III. SIMULATION AND EXPERIMENTS

Simulation and experiments are both performed in order to verify the characteristics of STGS in detecting 208 liter steel waste drum. Monte-Carlo method (GEANT) is used in calibration and detection simulation. Considering the attenuation of the filler materials being related with the energy of radioactive nuclide, Cr-51 (0.32 MeV), Cs-137 (0.662 MeV), Co-60 (1.333 MeV) are selected in the simulation. The experiments only use Cs-137 and Co-60 as the emission sources because of the lack of standard source of Cr-51. Three types of materials are used in experiment for the standard waste drum, polyurethane (0.3 g/cc), density wood (0.7 g/cc) and polyamide (1.2 g/cc).

The standard drum is 56 cm in diameter, about 85 cm in

(a) Two voxels by ER   (b) Two voxels by EA

(c) Four voxels by ER   (d) Four voxels by EA

Fig. 3. The division of annular voxels in the segment where ER, EA denote the division methods according to equal radius or equal area.

Fig. 4. The photograph of partial experimental facilities.

height. Figure 4 is the photograph of partial experimental facilities. In order to save the detection time in experiments, the standard waste drum only uses three segments where the radioactive sources are placed in the middle. The detector is Canberra's pin coaxial high-purity Germanium (HPGe) detector with the efficiency of 40%. The crystal with a diameter of 6.2 cm and length of 5.95 cm is wrapped by an aluminum layer with a thickness of 1.5 mm. The detector is housed in a cylindrical lead shield of 4 cm thickness and positioned at 53 cm away from the drum center. Before the detector, a lead collimator is placed where the diameter is 8 cm, a square hole is 6 cm in side length and 15 cm in long. According to the geometric dimension and position, detection efficiency (E) of ring sources is distributed as shown in figure 5 where r denotes the radius of the ring. The detection efficiency is affected by the filler materials and radioactive nuclides. When the density is 0.3 g/cc, the detection efficiency decreases with source radius. When source radius is large, only some points within the perspective of the collimator will exhibit the high detection efficiency, but the most points out of the perspective will have very low detection efficiency. When the density is small, the attenuation of materials is also small, which will leads to the average detection efficiency in large radius becoming smaller

than that positioned in drum center. On the contrary, detection efficiency in drum center will decrease quickly by attenuation when the material density becomes large to such as 1.2 g/cc. When the density is 0.7 g/cc, the curve of detection efficiency is comparatively flat. The detection efficiency of Cr-51 is larger than other two nuclides because the gamma rays emitted from this nuclide has the low penetration which leads to most gamma rays will be absorbed by HPGe crystal. Only when the density is 1.2 g/cc, detection efficiency of Co-60 becomes larger than
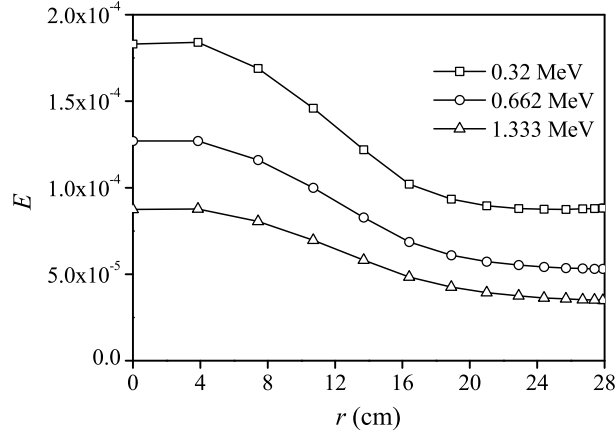
(a) Material density 0.3 g/cc
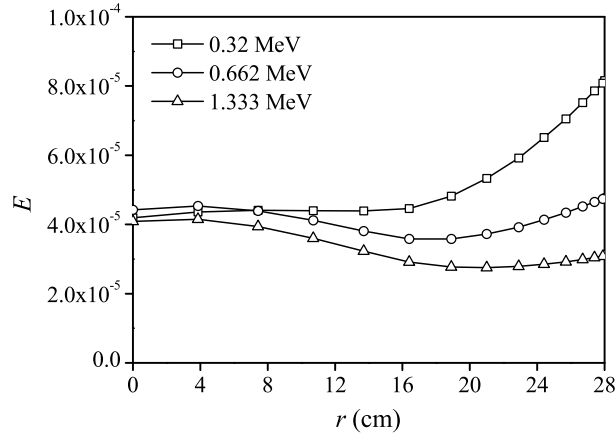
(b) Material density 0.7 g/cc
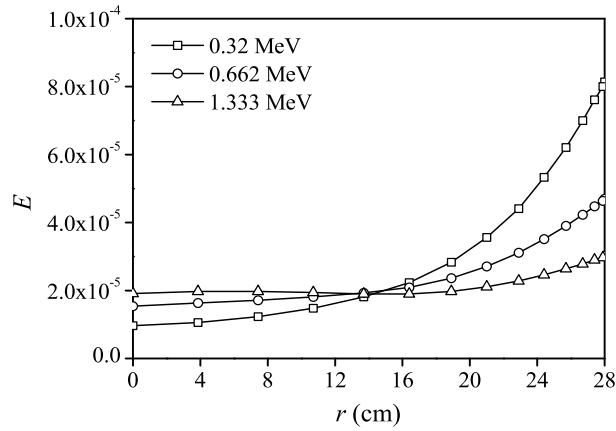
(c) Material density 1.2 g/cc
Fig. 5. The detection efficiency of the ring source versus its radius in the waste drum.

that of Cr-51 in drum center because gamma rays emitted by Cr-51 is attenuated much by the materials in waste drum.

In order to analyse the detection accuracy of STGS, SGS and STGS are compared. The waste drum is divided into 9 segments whose height is 10 cm. In each segment, four types of annular voxels are adopted in STGS as seen in figure 3. Accordingly, total four eccentric positions are selected in STGS, and the offset distance (Δy) is 0, 7, 14, 21 cm respectively. Among these measurements, one position of Δy=0 cm is used for SGS, two positions of Δy=0 and 14 cm are used for STGS with two voxels, and the total four positions are used for STGS with four voxels in one segment.

IV.   RESULTS AND DISCUSSION

Total activity is calculated by summing over all activities in the divided voxels. The reconstruction error (E_r) is defined as

$$E_r = \frac{A - A_{real}}{A_{real}} \times 100\% \qquad (7)$$

Where, A is the reconstructed activity of one nuclide, A_{real} is the real activity of the similar nuclide.

Cs-137 and Co-60 are used in the experiments, and their activities are about 20 μCi and 10 μCi respectively. Figure 6 shows the reconstruction error of the point emission source in experiments. In the figure, the symbol of 2 or 4 denotes the voxel number in each segment, ER or EA denotes the voxel
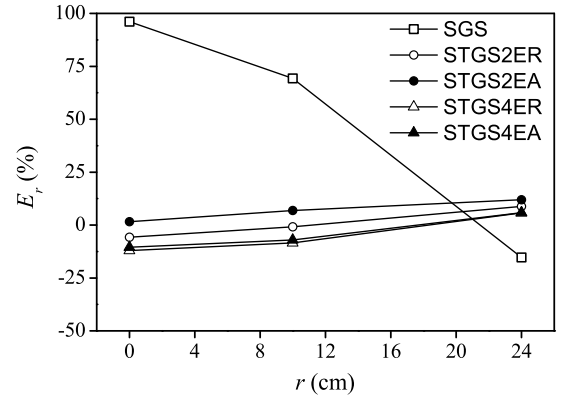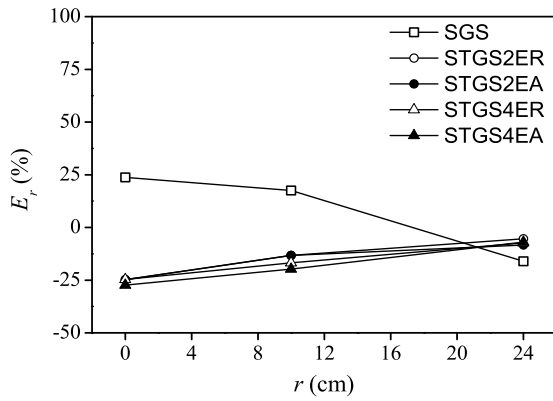

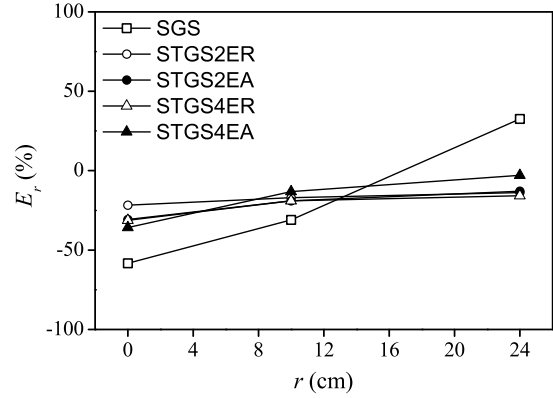(a) Cs-137 in the polyurethane material
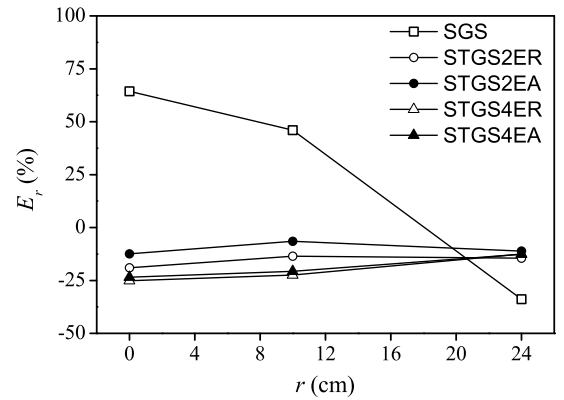
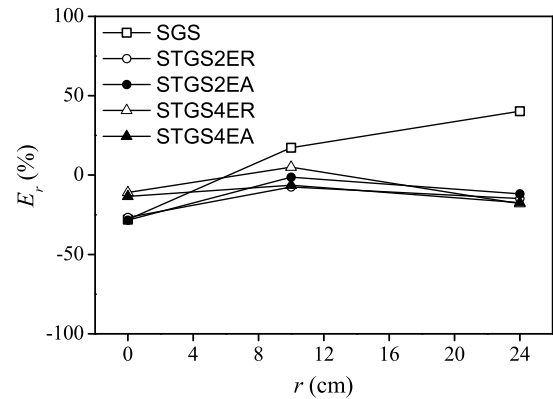(b) Co-60 in the polyurethane material
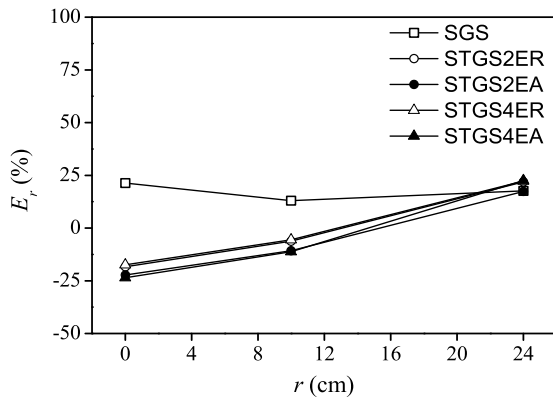
(c) Cs-137 in the density wood material

(d) Co-60 in the density wood material


(e) Cs-137 in the polyamide material

(f) Co-60 in the polyamide material

Fig. 6. The reconstruction results of one point emission source in experiments.

being divided according to equal radius or equal area. It can be found that SGS has a comparatively large reconstruction error, and the maximal reconstruction error reaches 100% for Cs-137 in the polyurethane material. The reconstruction error of SGS varies with the source radius and filler materials, for example it decreases with source radius in polyurethane material, but increases in polyamide material. The characteristics are related with the detection efficiency as shown in figure 5. According to the principle of SGS, the detection efficiency of one segment is the weighted average of all efficiencies distributed in each radius. If the average departs from the distributed efficiencies in a large degree, the large reconstruction error will appear and varies with real source radius.

Simulation supports 14 source positions and the construction results are shown in figure 7. Three nuclides of Cr-51, Cs-137 and Co-60 are adopted as emission sources. In the figure, the reconstruction errors is distributed similarly with experimental results. The error of SGS method is large and varies with source positions, especially in 0.3 g/cc and 1.2 g/cc materials.

STGS exhibits the comparatively low reconstruction error which is less than about 25% in both experiments and simulations. For the low density materials (0.3 g/cc), the reconstruction error of STGS is apparently small if compared with SGS and the other two densities. When the density is 0.7 g/cc, the reconstruction error is similar for both SGS and STGS because the error of SGS is small due to detection efficiency of point source varying within a narrow range.
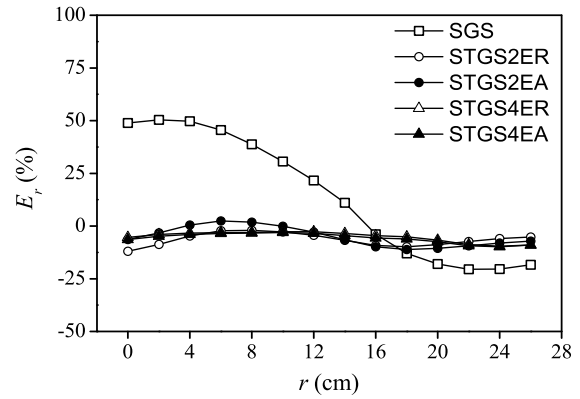
(a) Cr-51 in the material of 0.3 g/cc
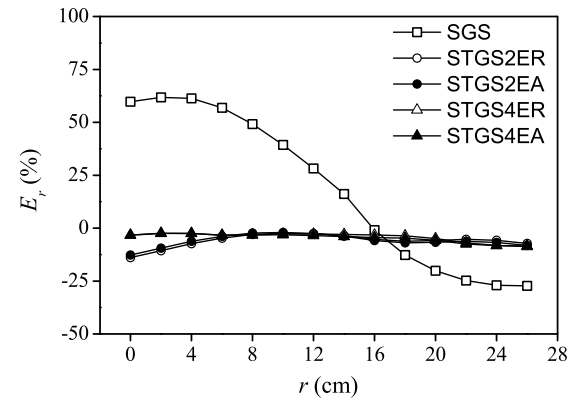
(b) Cs-137 in the material of 0.3 g/cc
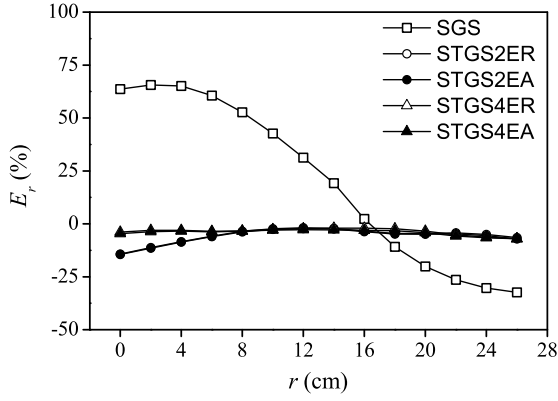
(c) Co-60 in the material of 0.3 g/cc

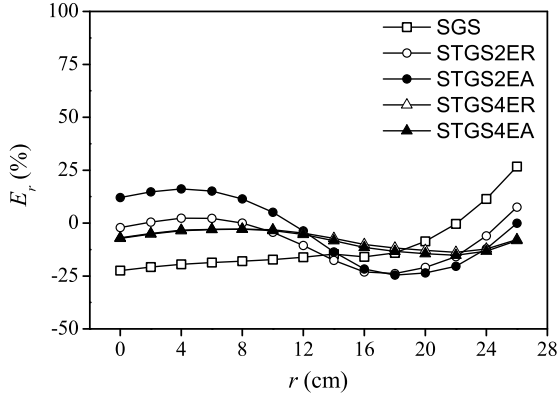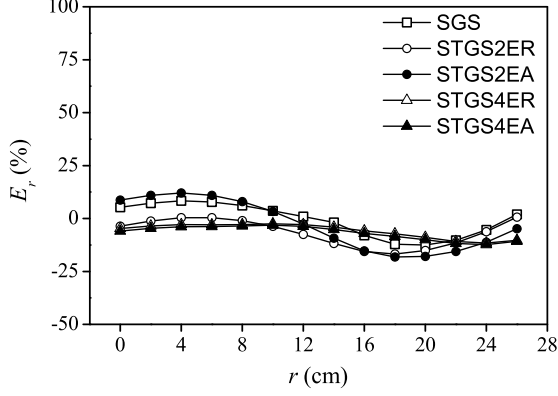(d) Cr-51 in the material of 0.7 g/cc

(e) Cs-137 in the material of 0.7 g/cc
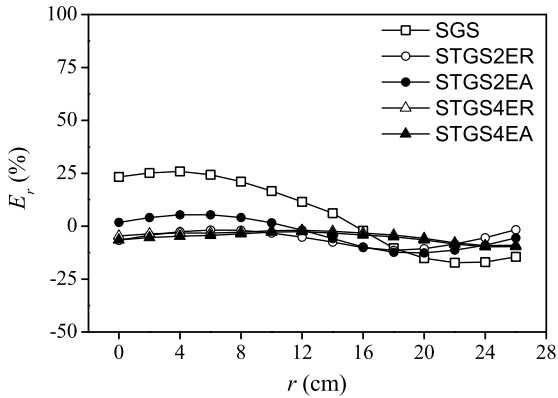
(f) Co-60 in the material of 0.7 g/cc
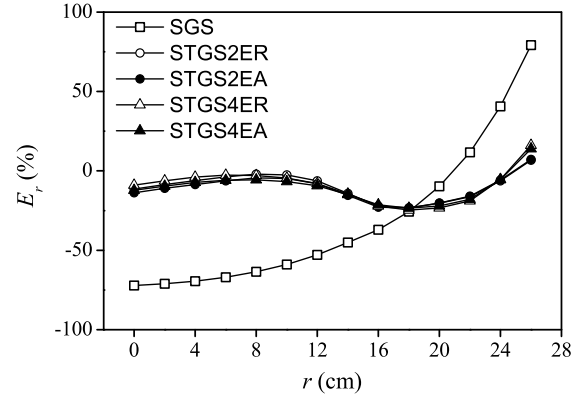
(g) Cr-51 in the material of 1.2 g/cc
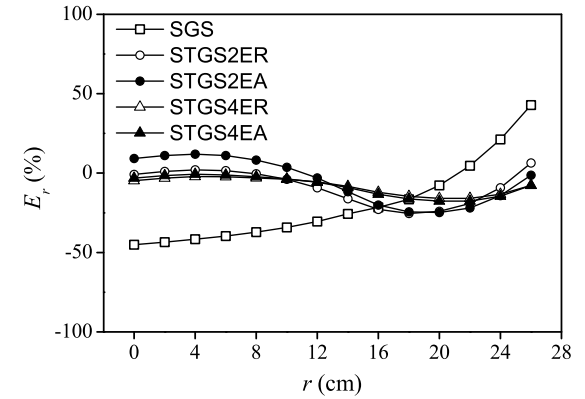
(h) Cs-137 in the material of 1.2 g/cc
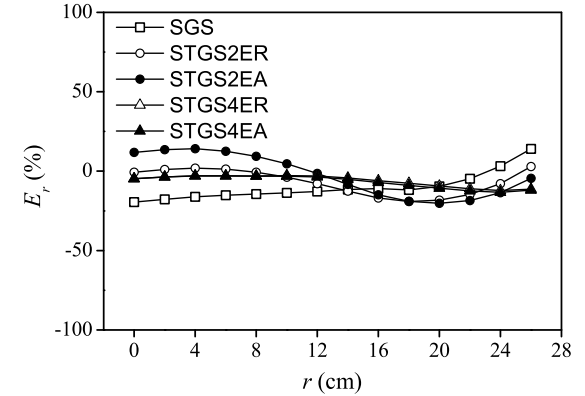
(i) Co-60 in the material of 1.2 g/cc

FIG. 7. The reconstruction results of one point emission source in simulation.

Statistical analysis is performed for the large number of reconstruction results. Besides the maximal and minimal reconstruction error, root mean square (RMS) of the error is defined to estimate the overall bias.

$$RMS = \sqrt{\frac{1}{N} \sum_{n=1}^{N} E_{r\,n}^{\,2}} \qquad (8)$$

Where N is the number of reconstruction error (E_r) adopted in statistical calculation.

As shown in table I, the reconstruction error of SGS method at the middle level density (0.7 g/cc) material is relatively small with absolute value less than 30%. If the density increases to

TABLE I. The statistical results for the point emission source in uniform filling material by simulation (unit %)

Density (g/cc)	Detection Type	Cr-51			Cs-137			Co-60		
		Min.	Max.	RMS	Min.	Max.	RMS	Min.	Max.	RMS
0.3	SGS	-20.51	50.41	31.83	-27.29	61.74	39.69	-32.36	65.57	42.58
	STGS2ER	-11.97	-2.00	7.07	-13.93	-2.39	6.72	-14.25	-1.89	6.54
	STGS2EA	-11.11	2.45	6.80	-12.74	-2.06	6.63	-14.49	-2.18	6.82
	STGS4ER	-9.56	-2.65	5.62	-8.75	-2.43	4.68	-7.09	-2.07	3.91
	STGS4EA	-9.82	-3.10	6.19	-8.43	-2.47	5.04	-7.02	-2.81	4.31
0.7	SGS	-22.47	26.73	17.18	-12.56	8.31	7.44	-17.23	25.85	17.84
	STGS2ER	-23.87	7.49	12.94	-16.78	0.67	9.05	-11.40	-1.63	6.66
	STGS2EA	-24.55	16.13	15.58	-18.15	12.04	11.65	-12.61	5.41	7.47
	STGS4ER	-13.78	-2.84	8.46	-11.61	-2.52	6.63	-9.14	-1.95	5.11
	STGS4EA	-15.24	-2.87	9.30	-17.66	-0.74	10.28	-9.71	-2.57	5.95
1.2	SGS	-72.20	79.21	54.82	-45.07	42.81	32.15	-19.48	14.10	13.25
	STGS2ER	-23.24	6.68	12.81	-25.42	6.32	13.63	-19.05	2.97	10.39
	STGS2EA	-23.50	7.19	13.59	-24.84	11.97	14.66	-20.20	14.10	13.09
	STGS4ER	-24.62	16.09	13.95	-15.86	-2.16	9.52	-12.18	-2.77	6.96
	STGS4EA	-23.46	13.86	14.01	-17.66	-0.74	10.28	-13.25	-3.00	7.71

TABLE II. The statistical results for the point emission source in nonuniform filling material by simulation (unit %)

Density Comb.	Detection Type	Cr-51			Cs-137			Co-60		
		Min.	Max.	RMS	Min.	Max.	RMS	Min.	Max.	RMS
Form 1	SGS	-47.5	70.71	36.06	-12.55	38.17	15.39	5.12	19.99	15.15
	STGS4ER	-34.04	23.72	20.54	-24.75	17.90	14.16	-18.02	13.18	10.16
Form 2	SGS	-32.82	32.23	25.05	-19.86	12.52	12.40	-15.66	34.53	20.23
	STGS4ER	-9.03	16.44	6.70	-3.07	12.97	4.24	-0.91	9.75	3.15
Form 3	SGS	-33.83	36.31	27.93	-20.86	14.56	11.65	-15.42	27.04	16.91
	STGS4ER	-2.57	21.30	12.12	0.43	16.65	9.09	1.82	12.50	6.95
Form 4	SGS	-26.18	44.39	21.33	-4.99	19.19	7.86	-5.93	31.17	18.90
	STGS4ER	-6.26	20.64	11.20	-4.38	15.55	7.32	-3.10	11.49	5.13

TABLE III. The statistical results for the point emission source in nonuniform filler materials by simulation (unit %)

Density (g/cc)	Detection Type	Cr-51			Cs-137			Co-60		
		Min.	Max.	RMS	Min.	Max.	RMS	Min.	Max.	RMS
0.3	SGS	-24.22	21.48	9.56	-25.96	24.81	10.53	-25.04	25.32	10.37
	STGS4ER	-5.68	3.61	2.26	-5.70	3.47	2.10	-5.13	3.23	1.84
0.7	SGS	-10.21	6.80	3.59	-16.33	12.16	5.84	-19.15	17.84	7.43
	STGS4ER	-8.15	5.03	3.00	-6.34	4.20	2.58	-5.56	3.83	2.18
1.2	SGS	-23.31	21.84	10.25	-10.76	9.50	4.65	-10.02	6.95	3.49
	STGS4ER	-16.00	14.49	5.59	-9.51	6.18	3.28	-6.45	4.33	2.64

1.2 g/cc, reconstruction error will depend on the type of nuclides. For example, reconstruction error is relatively low for the nuclide of Co-60 and high for Cr-51. This distribution is related with detection efficiency versus the source radius which depends on the attenuation of the filler material, penetrability of the gamma ray, the dimension of the collimator and position of the detector. In the present experimental conditions, the material density of 0.7 g/cc seems to the appropriate case for SGS with relatively high detection accuracy, especially for the nuclide of Cs-137. However, the accuracy of SGS is low in another material density, and the absolute maximal reconstruction error has exceeded 50% and RMS has exceeded 30% in most cases.

STGS has improved the detection accuracy effectively, and the absolute maximal reconstruction error of all cases is less than that of SGS. When the density is 0.3 g/cc, the absolute maximal reconstruction error is less than 15% and RMS is less than 8%, which is a quarter or less of SGS. When the density is 1.2 g/cc, the absolute maximal reconstruction error is less than 25% and RMS is less than 15%, which is almost a third of SGS for Cr-51 and Cs-137. Although the accuracy of SGS is

relatively high when the density is 0.7 g/cc, the absolute maximal reconstruction error and RMS of STGS are also less than that of SGS in most cases. If the four divisions of STGS are compared, the division of four voxels exhibits the better accuracy than that of two voxels, and the division of ER is slightly better than that of EA division.

In order to simulate the nonuniform material in the waste drum, two materials of 0.7 and 1.2 g/cc are selected to coexist in the segment with four combination forms as shown in figure 8. Table II lists the statistical results, and only the case of STGS4ER is selected because this case exhibits the best performance in the uniform material. In SGS, the reconstruction error of Cr-51 is relatively large especially in the nonuniform material of form 1, and the error of Cs-137 is the lowest between the three nuclides. At the same time, STGS improves the detection accuracy in the nonuniform materials. For example, the absolute maximal reconstruction error of Cr-51 is almost less than 25% and less than 18% for both Cs-137 and Co-60, RMS is smaller than SGS and especially decreases to half for Cr-51 and Co-60.

In addition to one point emission source, multi-point sources

(a) Form 1   (b) Form 2
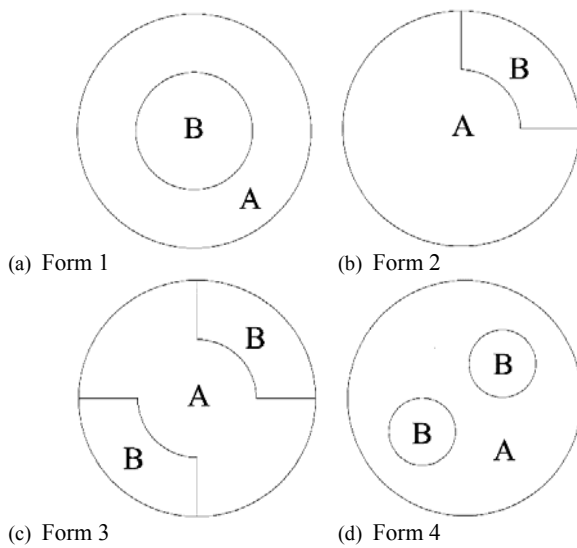
(c) Form 3   (d) Form 4

Fig. 8. The segmental layout of the filler with two materials where A represents the density of 0.7 g/cc and B represents the density of 1.2 g/cc.

simultaneously existing in the waste drum are simulated. Total 54 point sources, on average 6 sources in one segment are adopted including three nuclides of Cr-51, Cs-137 and Co-60 with random activities. The positions of all point sources are also randomly located in the waste drum. The reconstruction results are listed in table III. Compared with the case of one point source, the overall reconstruction error obviously decreases because the uniformity is reduced by using the multi-point sources. STGS has the better detection accuracy, and the absolute maximal error and RMS are both smaller than that of SGS. When the density is 0.3 g/cc, RMS of STGS is less than 2.5%, which is a quarter of SGS. When the density is 0.7 g/cc, RMS of STGS is less than 4%, while the maximal RMS of SGS is less than 7.5%. When the density is 1.2 g/cc, the maximal RMS of STGS is less than 6%, while the maximal RMS of SGS is less than 11%.

The above results show that STGS will improve the detection accuracy to the radioactive waste drum. The improvement is caused by STGS employing tomography to reconstruct the radial distribution of radionuclide and its activity in annular voxels instead of SGS assuming uniform distribution of the radioactive source. In order to colse the voxels in reconstruction calculation, more assay times are necessary for STGS, which will cause the detection time longer than SGS. However, the voxels' number of STGS is still much fewer than TGS, the measurement time will be shortened. It is concluded that STGS is an effective method having a good overall performance with relatively high detection accuracy and short measurement time if compared with SGS and TGS respectively.

V. CONCLUSION

One gamma scanning method and its algorithm, namely semi-tomographic gamma scanning (STGS) are proposed aiming at the low and intermediate level radioactive waste drum in order to improve the detection performance. Experiments and simulation are performed to verify the accuracy of this method which applies three types of nuclides, point source and multi-

point sources, uniform and nonuniform filler materials.

As to one point source in the uniform material, experimental and simulation results are consistent and proved that STGS has a very lower reconstruction error than SGS. The reconstruction error depends on the type of nuclides and filler materials. For the point source, the absolute maximal reconstruction error of STGS is less than 15% and RMS is less than 8% when density is 0.3 g/cc, and they are less than 25% and 15% for both density of 0.7 and 1.2 g/cc. For multi-point sources, the absolute maximal reconstruction error of STGS is less than 10% and RMS is less than 6% in most cases. For nonuniform material, the absolute maximal reconstruction error of STGS is less than 20% and RMS is less than 10% in most cases. If compared with SGS, the reconstruction error and RMS will be reduced by one quarter to one third or less for most cases.

The assumption of uniform distribution of emission sources in the segment is the core reason to cause SGS has a very large reconstruction error because the detection efficiency will be varied versus source radius. STGS uses tomographic method to reconstruct radial distribution of emission sources, which leads to the improvement of measurement accuracy. Although the detection time will be longer than SGS, STGS has a good overall performance that measurement accuracy is better than SGS and assay time is shorter than TGS.

REFERENCES

[1] E. R. Martin, D. F. Jones, J. L. Parker, "Gamma-ray Measurements with the Segmented Gamma Scan", Technical Report, Los Alamos Scientific Laboratory, 1977.
[2] R.J. Estep, T. H. Prettyman，and G. A. Sheppard, "Tomographic Gamma Scanning to Assay Heterogeneous Radioactive Waste," Nucl. Sci. and Eng., vol. 118, pp. 145-152, 1994.
[3] J. M. Kirkpatrick, J. M. Kirkpatrick, P.J. LeBlanc, D. Nakazawa, D. L. Petroka, S. Kane Smith, and R. Venkataraman, "A Mobile Automated Tomographic Gamma Scanning System – 13231," WM2013 Conference, February 24-28, Phoenix, Arizona USA, pp. 1-14, 2013.
[4] T. H. Anh, N. D. Thanh, and T. Q. Dung, "Evaluation of performance of a new gamma technique for assay of radioactive waste," Annals of Nuclear Energy, vol. 32, pp. 1516–1523, 2005.
[5] C. Liu, D. Z. Wang, Y. F. Bai, and N. Qian., "An improved segmented gamma scanning for radioactive waste drums", Nuclear Science and Techniques, vol. 2, pp. 204-208, 2010.
[6] Y.F. Bai, E. Mauerhofer, D.Z. Wang, and R. Odoj, "An improved method for the non-destructive characterization of radioactive waste by gamma scanning," Applied Radiation and Isotopes, vol. 67, pp. 1897–1903, 2009.
[7] T. Krings, and E. Mauerhofer, "Reconstruction of the activity of point sources for the accurate characterization of nuclear waste drums by segmented gamma scanning", Applied Radiation and Isotopes, vol. 69, pp. 880–889, 2011.
[8] C. Liu, W.G. Gu, N. Qian, D. Z. Wang, "Study of Image Reconstruction Using Dynamic Grids in Tomographic Gamma Scanning," Nuclear Science and Techniques. vol. 23, pp.277–283, 2012.
[9] W.G. Gu, C. Liu, N. Qian, D. Z. Wang, "Study on detection simplification of tomographic gamma scanning using dynamic grids applied in the emission reconstruction", Annual of Nuclear Energy. vol. 58, pp. 113–123, 2013.